

# Electron Capture Dissociation for Structural Characterization of Multiply Charged Protein Cations

Roman A. Zubarev, David M. Horn, Einar K. Fridriksson, Neil L. Kelleher, Nathan A. Kruger, Mark A. Lewis, Barry K. Carpenter, and Fred W. McLafferty\*

Department of Chemistry and Chemical Biology, Baker Laboratory, Cornell University, Ithaca, New York 14853-1301

**For proteins of <20 kDa, this new radical site dissociation method cleaves different and many more backbone bonds than the conventional MS/MS methods (e.g., collisionally activated dissociation, CAD) that add energy directly to the even-electron ions. A minimum kinetic energy difference between the electron and ion maximizes capture; a 1 eV difference reduces capture by 10<sup>3</sup>. Thus, in an FTMS ion cell with added electron trapping electrodes, capture appears to be achieved best at the boundary between the potential wells that trap the electrons and ions, now providing 80 ± 15% precursor ion conversion efficiency. Capture cross section is dependent on the ionic charge squared (z<sup>2</sup>), minimizing the secondary dissociation of lower charge fragment ions. Electron capture is postulated to occur initially at a protonated site to release an energetic (~6 eV) H<sup>•</sup> atom that is captured at a high-affinity site such as –S–S– or backbone amide to cause nonergodic (before energy randomization) dissociation. Cleavages between every pair of amino acids in mellitin (2.8 kDa) and ubiquitin (8.6 kDa) are represented in their ECD and CAD spectra, providing complete data for their de novo sequencing. Because posttranslational modifications such as carboxylation, glycosylation, and sulfation are less easily lost in ECD than in CAD, ECD assignments of their sequence positions are far more specific.**

Biomolecule sequencing by mass spectrometry (MS) and tandem MS (MS/MS) has been important for many decades and has been extended recently to large (>10 kDa) molecules such as proteins<sup>1</sup> and DNA.<sup>2</sup> Electrospray ionization (ESI) of a complex protein mixture yields their individual molecular ions, from which MS/MS spectra can be obtained on as little as 10<sup>-17</sup> mol of

protein.<sup>3</sup> Backbone fragmentation<sup>4–12</sup> of an ionized linear molecule T–AB...YZ–T' of known terminal groups T, T' can yield fragment ions such as T–A, T–AB, B...YZ–T', and Z–T', whose masses then define the backbone positions of the units A, B, etc.; for proteins, these units are the common amino acids. Assignment of an individual amino acid requires backbone cleavage on both sides of the residue, but for larger multiply charged proteins, only a small fraction (e.g., 25% for ubiquitin, 8.6 kDa) of the amino acids are separated by the common "heating" methods, collisionally activated dissociation (CAD),<sup>4</sup> infrared multiphoton dissociation (IRMPD),<sup>5</sup> blackbody infrared dissociation (BIRD),<sup>6</sup> surface induced dissociation,<sup>7</sup> inelastic electron collision (electron impact excitation of ions from organics, EIEIO),<sup>8</sup> and ion bombardment.<sup>9</sup> A complementary new method, electron capture dissociation (ECD),<sup>13</sup> causes different backbone cleavages that can nearly complete the MS sequence coverage. A more extensive descrip-

- (1) (a) Biemann, K. In *Methods in Enzymology*; McCloskey, J. A., Ed.; Academic Press: San Diego, 1990; Vol. 193 p 887. (b) McLafferty, F. W. *Acc. Chem. Res.* **1994**, *27*, 379–386. (c) Andersen, J. S.; Svensson, B.; Roepstorff, P. *Nature Biotechnol.* **1996**, *14*, 449–457. (d) Qin, J.; Chait, B. T. *Anal. Chem.* **1997**, *69*, 4002–4009. (e) Kuster, B.; Mann, M. *Curr. Opin. Chem. Biol.* **1998**, *8*, 393–400. (f) McLafferty, F. W.; Kelleher, N. L.; Begley, T. P.; Fridriksson, E. K.; Zubarev, R. A.; Horn, D. M. *Curr. Opin. Chem. Biol.* **1998**, *2*, 571–578. (g) McLafferty, F. W.; Fridriksson, E. K.; Horn, D. M.; Lewis, M. A.; Zubarev, R. A. *Science* **1999**, *284*, 1289–1290. (h) Jensen, P. K.; Pasa-Tolic, L.; Anderson, G. A.; Horner, J. A.; Lyston, M. S.; Bruce, J. E.; Smith, R. D. *Anal. Chem.* **1999**, *71*, 2076–2084.
- (2) Little, D. P.; Aaserud, D. J.; Valaskovic, G. A.; McLafferty, F. W. *J. Am. Chem. Soc.* **1996**, *118*, 9352–9359.

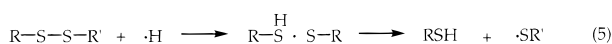
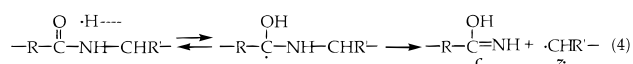
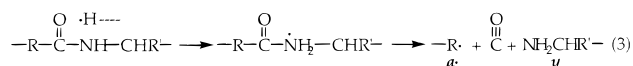
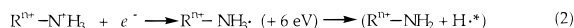
- (3) (a) Valaskovic, G. A.; Kelleher, N. L.; McLafferty, F. W. *Science* **1996**, *273*, 1199–1202. (b) Shabanowitz, J.; Settlage, R. E.; Marto, J. A.; Christian, R. E.; White, F. M.; Russo, P. S.; Martin, S. E.; Hunt, D. F. In *Mass Spectrometry in Biology and Medicine*; Burlingame, A. L., Carr, S. A., Baldwin, M. A., Eds.; Humana: Totowa, NJ, 1999.
- (4) (a) Loo, J. A.; Udseth, H. R.; Smith, R. D. *Rapid Commun. Mass Spectrom.* **1988**, *2*, 207–210. (b) Gauthier, J. W.; Trautman, T. R.; Jacobsen, D. B. *Anal. Chim. Acta* **1991**, *246*, 211–225. (c) Senko, M. W.; Speir, J. P.; McLafferty, F. W. *Anal. Chem.* **1994**, *66*, 2801–2808.
- (5) Little, D. P.; Speir, J. P.; Senko, M. W.; O'Connor, P. B.; McLafferty, F. W. *Anal. Chem.* **1994**, *66*, 2809–2815.
- (6) Price, W. D.; Schnier, P. D.; Williams, E. R. *Anal. Chem.* **1996**, *68*, 859–866.
- (7) (a) McCormack, A. L.; Jones, J. L.; Wysocki, V. H. *J. Am. Soc. Mass Spectrom.* **1992**, *3*, 859–862. (b) Chorus, R. A.; Little, D. P.; Beu, S. C.; Wood, T. D.; McLafferty, F. W. *Anal. Chem.* **1995**, *67*, 1042–1046.
- (8) Cody, R. B.; Freiser, B. S. *Anal. Chem.* **1979**, *51*, 547–551. Wang, B.-H.; McLafferty, F. W. *Org. Mass Spectrom.* **1990**, *25*, 554–556.
- (9) Wang, B.; Amster, I. J.; McLafferty, F. W.; Brown, I. G. *Int. J. Mass Spectrom. Ion Processes* **1990**, *100*, 51–61.
- (10) Schnier, P. D.; Jurchen, J. C.; Williams, E. R. *J. Phys. Chem. B* **1999**, *103*, 737–745.
- (11) McLafferty, F. W. In *Mass Spectrometry in the Analysis of Large Molecules*; McNeal, C. J., Ed.; John Wiley: New York, 1986; pp 107–120. McLafferty, F. W.; Amster, I. J.; Furlong, J. J. P.; Loo, J. A.; Wang, B. H.; Williams, E. R. In *Fourier Transform Mass Spectrometry: Evolution, Innovation, and Application*; Buchanan, M. V., Ed.; ACS Symposium Series 359; American Chemical Society: Washington, D. C., 1987; pp 116–126.
- (12) Guan, Z.; Kelleher, N. L.; O'Connor, P. B.; Aaserud, D. J.; Little, D. P.; McLafferty, F. W. *Int. J. Mass Spectrom. Ion Processes* **1996**, *157/158*, 357–364.
- (13) (a) Zubarev, R. A.; Kelleher, N. L.; McLafferty, F. W. *J. Am. Chem. Soc.* **1998**, *120*, 3265–3266. (b) Zubarev, R. A.; Kruger, N. A.; Fridriksson, E. K.; Lewis, M. A.; Horn, D. M.; Carpenter, B. K.; McLafferty, F. W. *J. Am. Chem. Soc.* **1999**, *121*, 2857–2862.

tion for ECD is given here, including details on related processes, mechanisms, instrumentation, and experimental procedures that increase ECD efficiency from  $\leq 27$  to  $80 \pm 15\%$ .

All of these "heating" methods show very similar selectivity for bond cleavages. All add internal energy to the large molecules at a much slower rate than that required for energy randomization, so that the weakest bonds are cleaved. Supporting this, Williams has recently shown<sup>10</sup> that the dissociations caused by BIRD and by CAD of molecular ions of the same temperature exhibit the same rate constants for eq 1 reactions. It had been proposed<sup>11</sup>

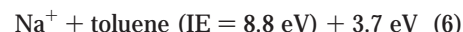


that dissociations that instead involve an odd-electron hypervalent species (e.g.,  $\text{R-NH}_3^{\cdot}$ ) could surmount this restriction. Serendipitously, that was effected first with 193 nm (6.4 eV) photons striking the cell walls to eject low-energy electrons;<sup>12</sup> their capture (ECD) leads to entirely different dissociation chemistry (eqs 2–5).<sup>13</sup>



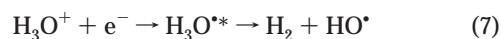
The most common "bottom up" approach to obtain MS sequence information from proteins is proteolysis to produce smaller ( $< 3$  kDa) peptides that are then sequenced by MS/MS.<sup>1</sup> Usually the proteolysis products only provide 40–90% sequence coverage, and ordering the peptide sequences in the protein usually requires one or more additional proteolysis/MS/MS events with other enzymes. An alternative "top down" strategy<sup>14</sup> has been applied to carbonic anhydrase (29 kDa) and several larger proteins.<sup>15</sup> Initial limited degradation (MS/MS or proteolysis) produces fragments sufficiently large so that the masses of one or more "complementary" sets sum to that of the whole molecule, providing complete coverage of the protein. The process is continued, dissociating each of the larger pieces to produce smaller complementary sets until the pieces are small enough for complete (or sufficiently extensive) sequencing. Thus, ECD could be a real advantage for top down sequencing if it provided as extensive sequencing at 10 kDa as is now possible at 2 kDa and if its  $\leq 27\%$  efficiency could be improved.<sup>13,16</sup>

**Electron Capture Methods.** For the technique discussed here as ECD, a multiply charged cation captures an electron to produce cationic dissociation products (eqs 2–5). However, a surprising variety of other MS-related techniques involve electron capture that can lead to dissociation. A neutral capturing a low-energy electron forms a negative ion, often one in a dissociative state.<sup>17</sup> In neutralization–reionization MS, a fast positive ion can capture an electron from a neutral species; the new neutral will be formed with sufficient internal energy to dissociate if the ionization energy (IE) of the  $e^-$  donating neutral is sufficiently lower than that of the product (eq 6).<sup>18</sup> Dissociative electron



transfer can even occur between neutrals in the condensed phase,<sup>19</sup> and anions can supply electrons in charge-transfer reactions with cations.<sup>20</sup>

The neutral product of eq 6 would be formed with even higher internal energy by capture of an electron (IE = 0.0 eV). These "dissociative recombination" reactions<sup>21</sup> have been extensively studied by physicists, even in high-energy ion storage rings, to provide detailed data on reactions important in interstellar chemistry, such as eq 7 that forms the unstable hypervalent



neutral  $\text{H}_3\text{O}^{\cdot}$ . Approximately 5 eV (IE of  $\text{H}_3\text{O}^{\cdot}$ ) is released in this neutralization; without dissociative dissipation of this energy in such a small species, autoionization to re-emit the  $e^-$  is probable.

However, for MS/MS the dissociation products must also be ions so that they can be mass analyzed; thus, multiply charged cations are required to yield cationic products on reduction. This was demonstrated by Beynon and co-workers in a pioneering study<sup>22</sup> of the "electron capture-induced decomposition" of benzene  $\text{C}_6\text{H}_6^{2+}$  ions of high kinetic energy (4 keV), whose collisions with benzene or rare gas atoms produce  $\text{C}_6\text{H}_6^{+\cdot}$  and minor amounts of its dissociation products. However, this does not fit the definition of ECD proposed here; collisions on lower IE targets resulted in lower internal energy  $\text{C}_6\text{H}_6^{+\cdot}$  ions,<sup>22</sup> in contrast to eq 6. Use of a free electron and no collisional energy should produce a large energy release of 16.8 eV (neglecting the Franck–Condon factor), as the IE required to produce  $\text{C}_6\text{H}_6^{+\cdot}$  and  $\text{C}_6\text{H}_6^{2+}$  ions are 9.2 and 26.0 eV, respectively. In a similar fashion, in EIEIO  $e^-$  capture does not occur; the inelastic collision of higher energy electrons with ions only imparts energy for dissociation.<sup>8</sup>

- (14) Kelleher, N. L.; Lin, H. Y.; Valaskovic, G. A.; Aaserud, D. J.; Fridriksson, E. K.; McLafferty, F. W. *J. Am. Chem. Soc.* **1999**, *21*, 806–812.  
 (15) O'Connor, P. B.; Speir, J. P.; Senko, M. W.; Little, D. P.; McLafferty, F. W. *J. Mass Spectrom.* **1995**, *30*, 88–93. Kelleher, N. L.; Nicewonger, R. B.; Begley, T. P.; McLafferty, F. W. *J. Biol. Chem.* **1997**, *272*, 32215–32220. Wood, T. D.; Guan, Z.; Borders, C. L., Jr.; Chen, L. C.; Kenyon, G. L.; McLafferty, F. W. *Proc. Natl. Acad. Sci. U.S.A.* **1998**, *95*, 3362–3365. Kelleher, N. L.; Taylor, S. V.; Grannis, D.; Kinsland, C.; Chiu, H.-J.; Begley, T. P.; McLafferty, F. W. *Protein Sci.* **1998**, *8*, 1796–1801.  
 (16) Kruger, N. A.; Zubarev, R. A.; Horn, D. M.; McLafferty, F. W. *Int. J. Mass Spectrom.* **1999**, *185/186/187*, 787–793.

- (17) Boesl, U.; Knott, W. *J. Mass Spectrom. Rev.* **1998**, *17*, 275–305.  
 (18) Gellene, G. L.; Porter, R. F. *Acc. Chem. Res.* **1993**, *16*, 200–207. McLafferty, F. W. *Int. J. Mass Spectrom. Ion Processes* **1992**, *192*, 221–225.  
 (19) Andrieux, C. P.; Saveant, J.-M.; Tardy, C. *J. Am. Chem. Soc.* **1998**, *120*, 4167–4175.  
 (20) Ogorzalek Loo, R. R.; Udseth, H. R.; Smith, R. D. *J. Phys. Chem.* **1991**, *95*, 6412–6415. McLuckey, S. A.; Stephenson, J. L.; Asano, K. G. *Anal. Chem.* **1998**, *70*, 1198–1202.  
 (21) Bates, D. R. In *Dissociative Recombination*; Rowe, B. R., Mitchell, J. B., Canosa, A., Eds.; Plenum Press: New York, 1993; pp 1–10.  
 (22) Vekey, K.; Brenton, A. G.; Beynon, J. H. *J. Phys. Chem.* **1986**, *90*, 3569–3577.

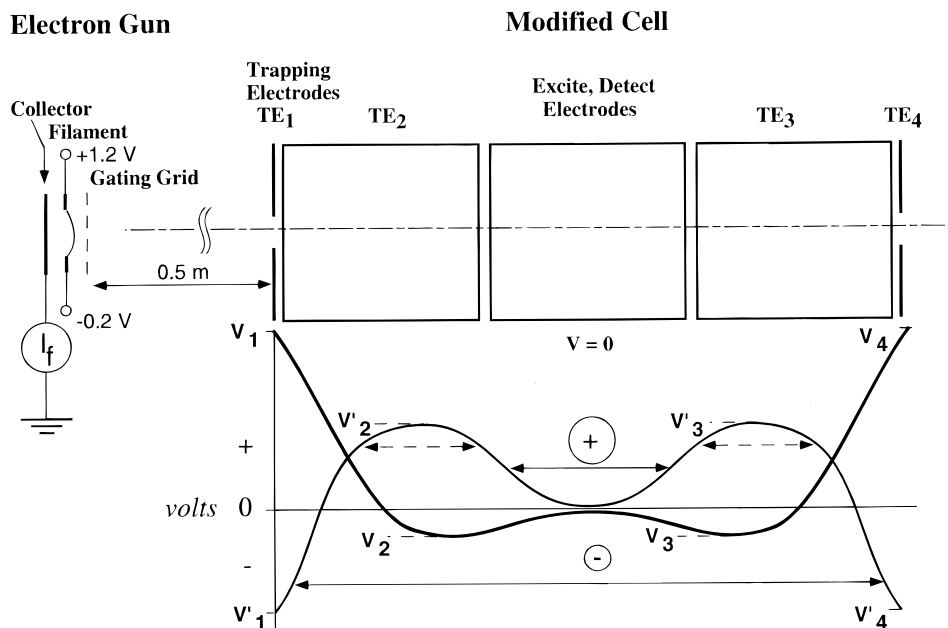


Figure 1. Schematic of the nested ion cell geometry used for ECD. The flat plate trapping electrodes TE<sub>1</sub> and TE<sub>4</sub> have been added outside the conventional cylindrical electrodes. The solid double-headed arrows correspond to the Z-axis oscillation amplitudes of positive ions and freshly captured electrons; after cooling, the latter occupy (dashed arrows) potential wells on either side of the positive ion well.

Our preliminary communications about ECD<sup>13,16,23</sup> are extended here to provide a more general picture, including instrumentation, high-efficiency operating procedures, overall spectral features, and amplification of mechanisms for H<sup>+</sup> capture (eqs 2–5) and nonergodic dissociation.

#### EXPERIMENTAL SECTION

Samples were obtained from Sigma, except for the 21-mer peptide graciously provided by Dr. Ted Thannhauser, Cornell DNA/Peptide Synthesis Facility. Samples were dissolved in 49:49:2 methanol/water/acetic acid mixture to 10<sup>-5</sup> M concentration and ionized by electrospray outside the instrument.

A modified Fourier transform (FT) mass spectrometer (6 T, Finnigan FTMS, Madison, WI) described previously<sup>24</sup> has been re-equipped with a conventional electron filament placed in the fringing magnetic field region, 0.5 m away from the cell.<sup>13</sup> This can be translated orthogonally to put it on-axis, or 5 mm off-axis when the IR laser is used for IRMPD.<sup>5</sup> Two extra copper disks (5.0 cm diameter) with an annular 8 mm hole were installed 1 mm outside at either end of the 5.65 cm diameter cylindrical trapping electrodes of the FTMS cell to create a nested geometry for simultaneous storage of oppositely charged species (Figure 1).<sup>25</sup>

ESI produces ions that are transported to the 10<sup>-9</sup> Torr region and captured in the cell by pulsing the buffer gas (Ar or N<sub>2</sub>, 10<sup>-6</sup> Torr for 20 ms). The desired charge state of positive ions is isolated by SWIFT<sup>26</sup> and dissociated. Typical ECD parameters

were as follows: filament current (measured at the collector 5 mm behind the filament)  $I_f = 0.3 \mu\text{A}$ ; bias of the electron filament center,  $V_f = +0.5 \text{ V}$  (termini,  $-0.2$  and  $+1.2 \text{ V}$ ); irradiation time, 3 s; voltage on the extra trapping plates,  $V_{1,4} = +3$  to  $+7 \text{ V}$ ; and voltage on the ion trapping cylinders  $V_{2,3} = -0.5 \text{ V}$  (Figure 1;  $V_{2,3} = -0.5 \text{ V}$  yields higher capture efficiency, but  $+1.0 \text{ V}$  yields higher fragment ion intensity). The center cylindrical electrode is grounded. A buffer gas was pulsed at the start of electron irradiation; argon was used for single and N<sub>2</sub> (higher pumping speed) for multiple spectral measurements.

Unless stated otherwise, ECD spectra reported here were obtained under these conditions. Far higher efficiencies are now obtainable with a modified procedure employing trapping voltages related as  $V'_{1-4}$  (Figure 1), filament termini  $-3$  and  $+4 \text{ V}$ , and multiple electron introduction events, without a cooling gas pulse, for ECD of the same ions. For example,  $80 \pm 15\%$  ECD efficiency was obtained for ubiquitin 12+ ions by admitting electrons ( $I_f = 0.3 \mu\text{A}$ ) into the cell of trapped ions for 3 s with  $V'_{1,2,3} = +1 \text{ V}$  and  $V_4 = -1 \text{ V}$ , capture of trapped e<sup>-</sup> for 6 s with  $V'_{1,4} = -1 \text{ V}$  and  $V_{2,3} = +1 \text{ V}$ , and ejection of the remaining electrons from the cell by setting  $V'_{1,4} = +2 \text{ V}$  for 0.5 s. This electron irradiation and capture cycle is then repeated 10 times with the same ions still trapped by  $V'_{2,3} = +1 \text{ V}$ . After this, on-resonance excitation is used to eject the remaining precursor ions, and the spectrum is measured. However, relative ion abundances are day-to-day variable, and optimum conditions should be determined for the specific ion species, electrospray conditions, precursor ion excitation and focusing, etc.

Dissociation by SORI-CAD<sup>4c</sup> and IRMPD<sup>5</sup> was performed as previously described. Mass spectra were recorded starting from  $m/z$  500 for proteins and  $m/z$  400 for peptides. The  $m/z$  scale was calibrated using bovine ubiquitin ( $M_r = 8564.63\text{-}5$ ); the italicized final digit denotes the mass difference (units of 1.002 35

- (23) Kruger, N. A.; Zubarev, R. A.; Carpenter, B. K.; Kelleher, N. L.; Horn, D. M.; McLafferty, F. W. *Int. J. Mass Spectrom.* **1999**, *182/183*, 1–5.  
 (24) Beu, S. C.; Senko, M. W.; Quinn, J. P.; Wampler, F. W., III; McLafferty, F. W. *J. Am. Soc. Mass Spectrom.* **1993**, *4*, 557–565.  
 (25) Wang, Y.; Malek, R.; Wanczek, K.-P. *Int. J. Mass Spectrom. Ion Processes* **1996**, *157/158*, 199–214.  
 (26) Marshall, A. G.; Wang, T. C. L.; Ricca, T. L. *J. Am. Chem. Soc.* **1985**, *107*, 7893–7898.

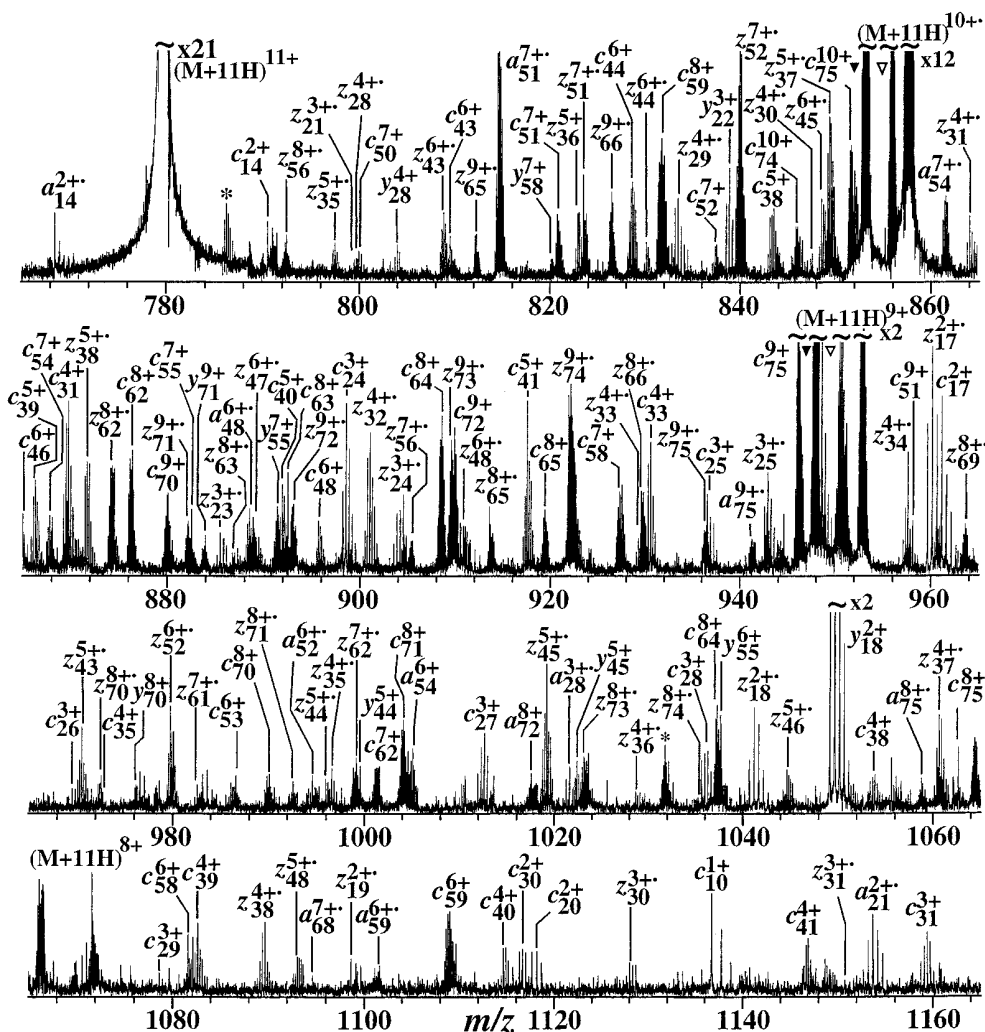


Figure 2. ECD spectrum of 11+ ions from bovine ubiquitin, 70 scans. Fragment ion designations from eqs 2 and 3; ▼, ▽: small neutral losses.

Da)<sup>27</sup> between the most abundant and monoisotopic peaks.<sup>1b</sup> Analyses were performed using the THRASH method programmed in PV-Wave.<sup>27</sup> For calculation of ECD efficiencies, normalized intensities of ion peaks (proportional to the number of ions of a particular kind in the cell) were determined as a sum of all isotopic peak intensities divided by the charge state of ions.

## RESULTS AND DISCUSSION

Exposing SWIFT-isolated<sup>26</sup> (M + 11H)<sup>11+</sup> ions from ESI of ubiquitin (8.6 kDa) to low-energy electrons produced the complex spectrum of Figure 2 containing 196 isotopic clusters. Note first the *m/z* values of most products versus that of the (M + 11H)<sup>11+</sup> precursor ions. Their energetic cleavage (CAD, IRMPD, etc.) would produce two primary products whose masses sum to 8.6 kDa and whose charges sum to 11+, so that their *m/z* values would be above and below the *m/z* value of the precursor. However, 178 of these 196 isotopic clusters in Figure 2 have higher *m/z* values, consistent with dissociation accompanied by loss of charge. This is borne out by the mass values of the molecular

ions formed with lower charge. As an extreme example, (M + 8H)<sup>8+</sup> ions of ubiquitin exposed to low-energy electrons give 5+ molecular ions; these are of 3 Da greater mass, (M + 8H)<sup>5+</sup>, than those from direct ESI to produce (M + 5H)<sup>5+</sup> (Figure 3). These products are consistent with electron capture as the initial event leading to dissociation (ECD).<sup>13</sup> The product ions are those predicted by eqs 3 and 4. Such *c* ions (eq 3) have been observed in in-source MALDI fragmentation,<sup>28</sup> and so those could arise by ECD as well.

As further illustrations, Figures 4–7 show, respectively, the ECD spectra of a 21-mer peptide, of cytochrome *c* (12.3 kDa), of apomyoglobin (17 kDa), and of carbonic anhydrase (29 kDa). With increasing size, the proportion of interresidue bonds cleaved by ECD decreases; there are 16/20 for the 21-mer, 67/75 for ubiquitin; 75/103 for cytochrome *c*, 30/152 for apomyoglobin, and none (of 258) for carbonic anhydrase ions. The latter 34+ ions only form the reduced molecular ion species (M + 34H)<sup>31–33+</sup>, and similar results are found for ECD of 49 kDa protein ions.<sup>13b</sup> For the 12 kDa and smaller ions, ECD has cleaved many more backbone bonds than CAD or IRMPD. ECD is also more effective

(27) Horn, D. M.; Zubarev, R. A.; McLafferty, F. W. *J. Am. Soc. Mass Spectrom.*, in press.

(28) Reiber, D. C.; Grover, T. A.; Brown, R. S. *Anal. Chem.* **1998**, *70*, 673–683.

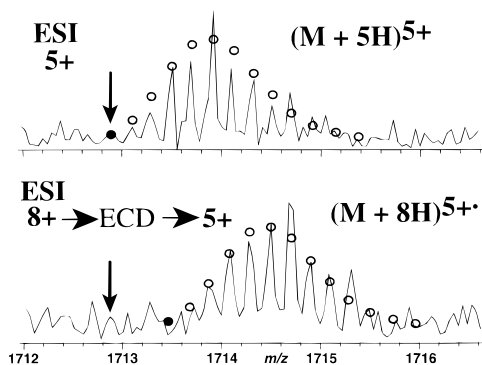


Figure 3. Isotopic peak abundances from ESI of ubiquitin. Top: Directly generated 5+ ions; bottom: 5+ ions from ECD reduction of (M + 8H)<sup>8+</sup> ions. Open circles, best fit of theoretical isotopic abundances; closed circle, monoisotopic mass.

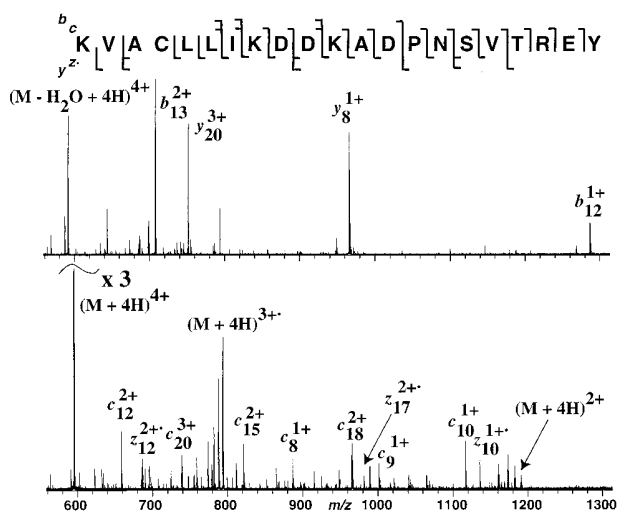


Figure 4. CAD (upper) and ECD (lower) spectra of ESI-generated (M + 4H)<sup>4+</sup> ions of a 21-mer peptide. Top: vertical shorter bars, ECD c, z cleavages; longer bars, IRMPD and CAD b, y cleavages.

with ions of low charge state; ubiquitin 7<sup>+</sup> ions show little dissociation by CAD<sup>4c</sup> or IRMPD,<sup>5</sup> but ECD provides extensive sequence information.

**ECD Experimental Procedures.** Electrons were produced by a conventional electrically heated filament on the side of the ion cell opposite to that for ESI ion introduction (Figure 1). An extra set of trapping electrodes for improved electron containment was installed on the outside (along the magnetic axis) of the cylindrical electrodes that normally trap the multiply charged positive ions formed by ESI within the grounded center cylindrical electrode.

**Effect of Electron Energy.** Using the (M + 15H)<sup>15+</sup> ions from cytochrome *c* (Figure 8) with filament currents of  $I_f = 0.33$  and  $1.0 \mu\text{A}$ , the cross section ( $\sigma$ ) value was measured at different  $V_f$  values, where  $\sigma$  is the ratio of relative reduction in intensity ( $\log_e I/I_0$ , peak heights) of the precursor ions divided by electron current passing through the cell (measured on the rods of the quadrupole just past the cell).  $V_f$  is the voltage at the center of the filament, differing by  $\sim 0.7$  V from the end values, which produces a broad spread of  $e^-$  energy values. Electrons can only leave the filament at negative local voltages, so the asymptotic approach to  $\sigma = 2 \times 10^{-11} \text{ cm}^2$  should represent the value for

near-zero energy electrons as  $I_f$  approaches zero. The collision cross section for neutrals with a 15<sup>+</sup> cytochrome *c* is  $2.5 \times 10^{-13} \text{ cm}^2$ .<sup>29</sup>

Observed values (Figure 8) are  $\sigma = \sim 10^{-11} \text{ cm}^2$  at  $V_f = 1.0$  V,  $3 \times 10^{-13}$  at 0.5 V, and  $\sim 10^{-14}$  at 0.0 V;  $\sigma$  is reduced by  $\sim 30$  and by  $\sim 10^3$  at electron energies of  $\sim 0.5$  and  $\sim 1.0$  eV. This is consistent with theory; the Thomson radius  $r$  is the distance at which the ionic electrostatic potential is equivalent to the electron energy,<sup>30</sup> making capture possible, and thus  $\sigma$  should be a function of  $r^2$ .

This ECD requirement for a near-zero translational energy difference between the ions and electrons presents a challenge for its implementation on other types of mass spectrometers. In radio frequency ion traps the stored ions have translational excitation as high as 5 eV, and electrons will also be excited by the rf fields. For magnetic sector and time-of-flight instruments,  $e^-$  capture could be effected before ion acceleration or by matching the electron velocity to that of the ions, as already demonstrated in ion storage rings.<sup>21</sup>

**Effect of Ionic Charge.** Relative electron capture efficiencies were compared for a mixture of  $z = 1+$  ions of gramicidin S, 5<sup>+</sup> ions of porcine insulin (5.8 kDa), and 15<sup>+</sup> ions of apomyoglobin (16.9 kDa) (Figure 9). Within experimental error,  $\sigma$  is dependent on  $z^2$ ;  $r$  should be a linear function of  $z$  if  $z$  is considered as a point charge, consistent with  $\sigma$  dependent on  $z^2$ . The point charge assumption is a fair approximation; in a separate experiment,  $\sigma$  for the 4<sup>+</sup> ions of insulin (5.8 kDa) was 20% higher than  $\sigma$  for the 4<sup>+</sup> ions of mellitin (2.8 kDa). With no positive charge,  $\sigma_{\text{max}}$  for  $e^-$  capture by neutral SF<sub>6</sub> is  $\sim 10^{-15} \text{ cm}^2$ .<sup>30b</sup>

In keeping with this effect of charge, secondary internal product ions are of very low abundance in ECD spectra that still contain a significant abundance of precursor ions. Further, for ECD it is best to select one or only a few charge states of a precursor; for simultaneous ECD of 8<sup>+</sup> through 13<sup>+</sup> of ubiquitin,  $\sigma(13+) = 2.6\sigma(8+)$ , and also 8<sup>+</sup> undergoes far less dissociation because of its lower electrostatic charge repulsion.

**Dissociation Extent versus Electron Energy.** The electrons admitted to the cell were restricted to those of higher kinetic energy by setting  $V_1 = -0.4$  V and  $V_4 = 0$ . Comparing an ECD spectrum of 11<sup>+</sup> ubiquitin ions to that of  $V_1 = 0$  V and  $V_4 = -0.4$  V showed no significant differences in the fragmentation pattern, although the ECD efficiency of the latter was 50% higher. This difference is consistent with both favored capture when translational energy of the electrons and ions differs by  $\ll 0.4$  eV and the fact that  $e^-$  capture releases far more energy,  $\sim 6$  eV (vide infra) than that of the  $e^-$  collision.

**Experimental Factors Influencing ECD Spectra.** Wanczek<sup>25</sup> has made a detailed study of the problems of storing and interacting species of both positive and negative charge in an ICR cell, with designs such as Figure 1. Basically, the ESI ions on passing TE<sub>4</sub> and entering the cell from the right lose kinetic energy by collisions with the pulse gas and so are trapped between the positive voltages on  $V_1$  and  $V_4$ . Making  $V_2$  and  $V_3$  negative ( $-0.5$  V) now makes a corresponding negative well between them for electrons in the center of the cell; after entering from the left and

(29) Chen, Y.-L.; Collings, B. A.; Douglas, D. J. *J. Am. Soc. Mass Spectrom.* **1997**, *8*, 681–687.

(30) (a) Thomson, J. J. *Philos. Mag.* **1924**, *47*, 337–378. (b) McDaniel, E. W. *Collision Phenomena in Ionized Gases*; Wiley: New York, 1964.

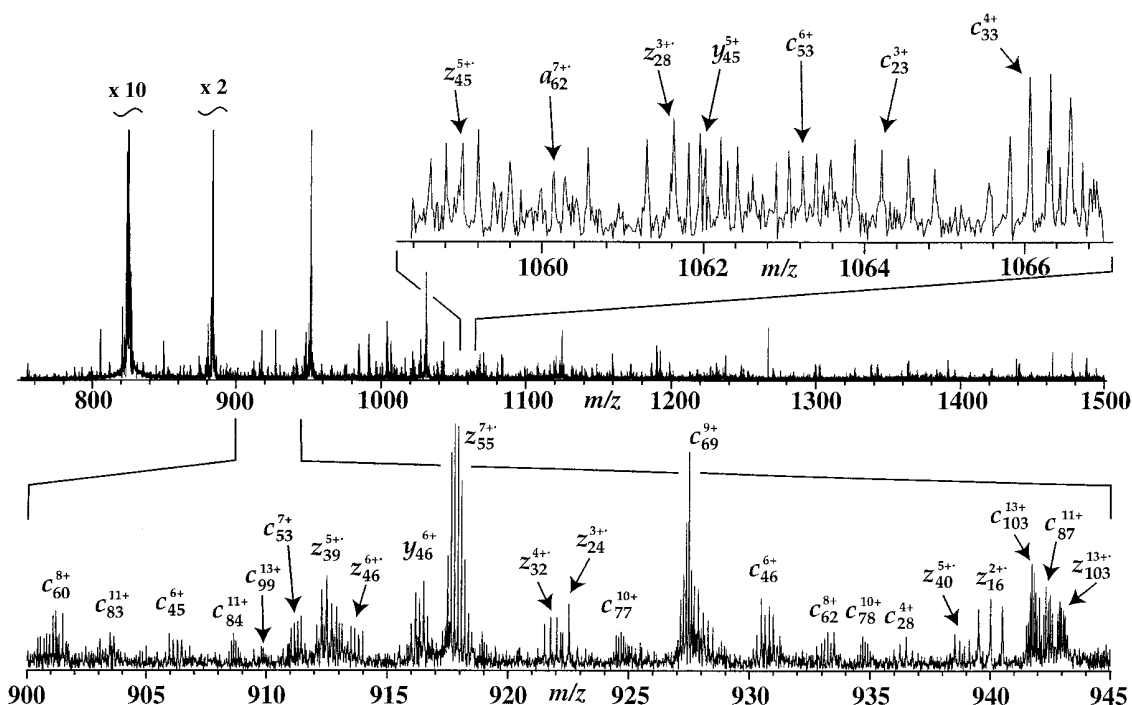


Figure 5. ECD spectrum of 15+ ions from cytochrome c.

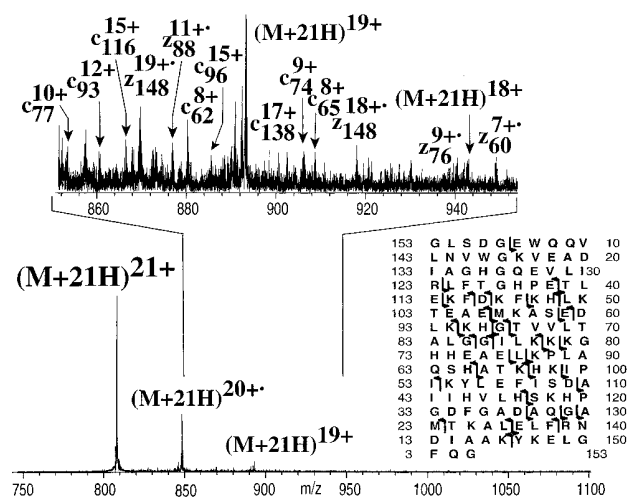


Figure 6. ECD spectrum of 21+ ions from apomyoglobin, 33 scans.

undergoing sufficient collisional cooling, they will be trapped in this well. Ions will first traverse the full area between  $TE_1$  and  $TE_4$ , but their kinetic energies will be  $>0.5$  eV when they are in the area between  $TE_2$  and  $TE_3$  that contains the electrons. However, when the ions are cooled to  $<0.5$  eV, they will be more narrowly confined in the negative potential wells of  $TE_2$  and  $TE_3$  on either side of the reverse potential well that confines the electrons. Now at the boundaries between these potential wells, both the ions and electrons must slow to zero energy before reversing course, an optimum condition for electron capture for an ion/electron pair whose maximum  $Z$ -axis kinetic energies sum to 0.5 eV. However, when the ions cool to kinetic energies near thermal within their potential wells, they will separate at the well bottoms where they can only interact with electrons that turn around at those specific  $Z$ -axis locations. These are electrons whose maximum kinetic energy is 0.5 eV; those of higher energy

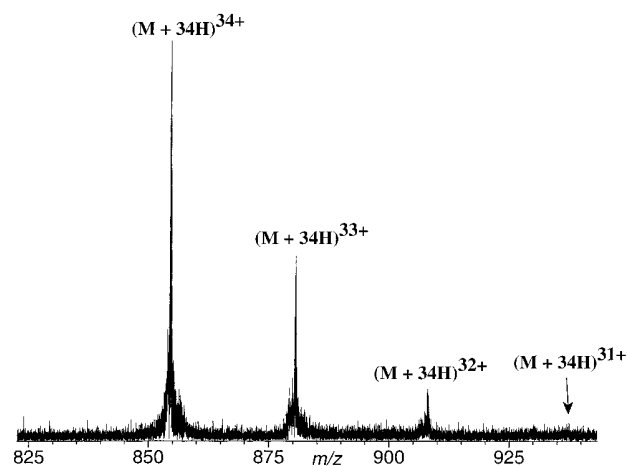


Figure 7. ECD spectrum of 34+ ions from carbonic anhydrase B.

escape and those of lower energy will not oscillate far enough to reach the trapped ions. This offers an explanation for earlier experimental results<sup>13a</sup> in which the maximum ECD efficiency was reached with only 60–70% reduction of the precursor ion intensity; the remaining ions presumably had become too cool to be accessible to low-energy electrons. Efficiencies measured were 10–25%, with a maximum of 27% observed, due both to incomplete reduction and to ion loss.

The initial  $X$ – $Y$  axis position of the electrons depends on from what part of the filament they are emitted, while for the ions the  $X$ – $Y$  axis positions are similarly dependent on the ion optics. A 7 s delay after SWIFT selection of the precursor ions before ECD produces 40% more  $e^-$  capture than no delay, probably due to ion translational cooling. Over two years of experience indicates, not surprisingly, that ECD efficiency and spectra are only qualitatively reproducible over weeks of time. For new samples, major

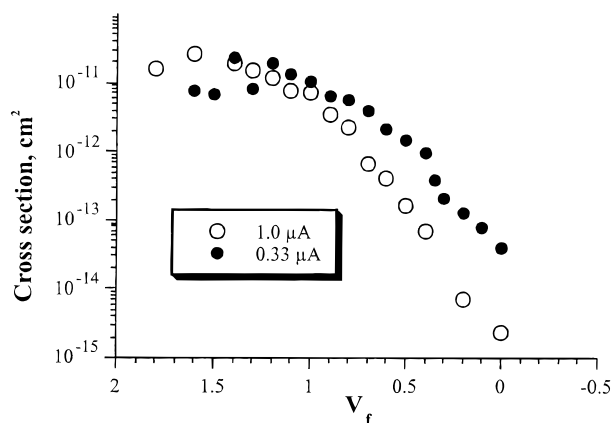


Figure 8. Effect of measured voltage at the filament center on observed electron capture cross section for electron beam currents of 0.33 and 1.0  $\mu\text{A}$ . Zero electron energy corresponds (see text) to  $V_f = \sim +1.2$  V.

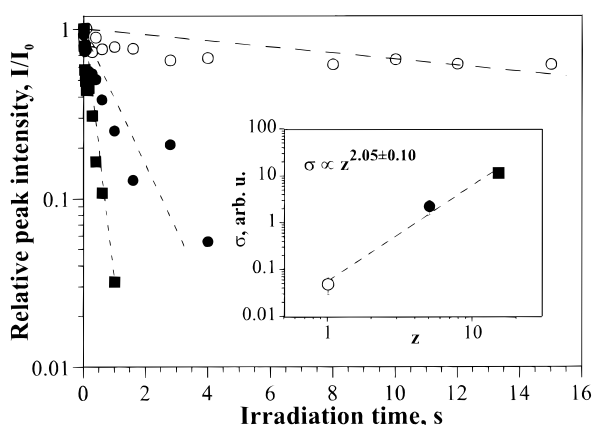


Figure 9.  $(M + nH)^{n+}$  abundance as a function of electron exposure time for gramicidin S 1+ (open circles), porcine insulin 5+ (closed circles), and apomyoglobin 15+ (squares) ions. Inset: relative electron capture cross sections versus charge.

experimental parameters should be optimized if ECD efficiency is important.

Electron irradiation for  $>3$  s appeared to decrease electron capture. Opening the electron gating grid greatly increases the current of the filament, causing it to become increasingly bright. Possibly the greatly increasing electron flow, or even the IR radiation, removes product ions from the cell. An additional grounded grid between the filament and gating grid does alleviate, but does not eliminate, this problem.

Several experimental adjustments gave little improvement. The electron current ( $I_f$ ) behind the filament is 3 times the current that reaches the quadrupole on the opposite side of the grounded cell; with the filament at  $-5$  V to increase the  $e^-$  energy and floating the ion cell to give the same potential difference increased the  $e^-$  current through the cell but did not improve the ECD spectra. Similarly, storing the electrons for 1 s in the magnetic field had no positive effect, even though other studies indicate that this is enough time for extensive radiative cooling.<sup>31</sup>

The efficiency of  $c$ ,  $z$  formation was increased by  $\sim 20\%$  using Ar instead of  $N_2$ , but Kr had no noticeable additional effect. The

(31) Li, G.-Z.; Guan, S.; Marshall, A. G. *J. Am. Soc. Mass Spectrom.* **1997**, *8*, 793–800.

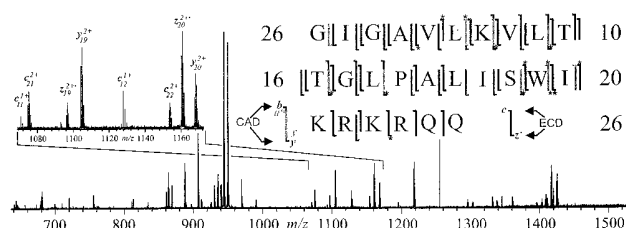


Figure 10. “High-efficiency” ECD spectrum and cleavages (shorter vertical bars) and CAD/IRMPD cleavages (longer vertical bars) of ESI-produced mellitin  $(M + nH)^{n+}$  ions. Cleavages with asterisks are data from other ECD spectra.

gas pulse can cool translationally excited ECD fragment ions, reducing their loss, as well as cooling the precursor ions and electrons. However, in the new procedure (vide infra) no gas pulse is used for electron cooling.

**Anion Exchange.** Use of the heavier  $SF_6$  in place of  $N_2$  or Ar lowered the ECD product yield from ubiquitin 11+ ions by a factor of  $\sim 8$ . A strong  $SF_6^-$  ( $m/z$  146) peak was observed, again indicative of a high proportion of low-energy electrons; the maximum  $e^-$  capture cross section of  $SF_6$  is at 0.08 eV.<sup>30b</sup> Anion-cation reaction rates<sup>20</sup> are several orders of magnitude slower than those for electron/cation;<sup>21</sup> 30 s storage of  $SF_6^-$  with the 11+ ubiquitin ions did produce near-normal  $e^-$  capture levels yielding reduced molecular ions, but with negligible ( $\sim 1\%$ )  $c$ ,  $z$  production. This is further evidence for the importance of the excitation energy ( $\sim 6$  eV) supplied in electron capture (vide supra); for charge exchange by  $SF_6^-$ , the excitation would be lowered by the  $SF_6$  electron affinity value of 1.1 eV<sup>32</sup> and also by the closer approach of  $SF_6^-$  before  $e^-$  transfer.

**ECD without Extra Electrodes.** Zubarev and co-workers reported<sup>33</sup> satisfactory spectra without use of the extra trapping plates. To simulate their absence, the original optimal settings ( $V_{1,4} = +3$  V;  $V_{2,3} = -0.5$  V) were changed to  $V_{1-4} = +1$  V; the electron capture efficiency was reduced by 30%. Similar results were obtained for grounded extra electrodes ( $V_{1,4} = 0$  V;  $V_{2,3} = +1$  V). However, further optimization without the extra electrodes was not investigated using the new high-efficiency methodology described below.

**High-Efficiency ECD.** In recent experiments (e.g., Figure 10), the same set of trapped ions in the cell is exposed to electrons multiple times, without a thermalizing gas pulse, trapping the electrons instead between the outer electrodes  $TE_1$  and  $TE_4$  (Figure 1). The ESI ion capture event is the same, with high positive charges on  $V_{1,4}$ ; the  $V_{2,3}$  electrodes are then raised to +1 V to squeeze the ions into the central grounded cylindrical electrode. During a 3 s electron beam-on event, electrode  $V_1$  is set to +1 V to admit the lowest energy electrons, while  $V_4 = -1$  V to force lower energy electrons back through the cell. The electron gating grid is shut, and the  $V_1$  potential is changed to  $-1$  V to force the remaining trapped electrons to oscillate repeatedly through the ion cloud; those cooled to a Z-axis kinetic energy of  $<1$  eV will then oscillate in the potential energy wells  $TE_2$  and  $TE_3$ . As discussed above, these will have the highest

(32) Rosenstock, H. M.; Draxl, K.; Steiner, B. W.; Herron, J. T. *J. Phys. Chem. Ref. Data* **1977**, *6* (Suppl. 1).

(33) Mirgorodskaya, E.; Roepstorff, P.; Zubarev, R. *Anal. Chem.* **1999**, *71*, 4431–4436.

capture probability during the near-zero energy “turn around” at the boundaries of the ion potential well in the center. The availability of the ions across the 0–1 V range of boundary sites will be greatly increased if the ions are translationally re-excited for each electron exposure event; this excitation apparently results from interaction with the new pulse of higher energy electrons and/or the shift in the ion potential well boundaries caused by changing  $V_1$  from +1 V to –1V. For ubiquitin 12+ ions, the optimum time for this secondary exposure to electrons was found to be 6 s, repeating the 3 s electron irradiation and 6 s exposure cycle 10 times for one set of trapped ions and ejecting any remaining electrons from the cell between each cycle. These new settings for the trapping electrodes also leave the cooled product ions in the cell center, an optimum condition for their subsequent measurement. Under conditions after ECD in which substantial amounts of precursor ions are still in the cell, on-resonance ejection of these ions improves the signal/noise of the measured spectrum by lowering the space charge.

Capture efficiencies of  $80 \pm 15\%$  were achieved for separate ECD spectra of the 11+, 12+, and 13+ ions of ubiquitin and ~60% for the 5+ ions of mellitin (Figure 10). Note that these are improved mainly in signal/noise and are qualitatively similar in fragmentation patterns. Although further studies, in progress, will check ECD efficiencies for a variety of proteins, efficiencies for those of ~10 kDa should be comparable to those of CAD (up to 92%)<sup>4c</sup> or IRMPD (up to 80%).<sup>5</sup>

**ECD Reaction Mechanisms.** It has been proposed<sup>13</sup> that ECD involves intramolecular transfer of a  $H^+$  atom with sufficient energy to cause dissociation, even at relatively distant sites, before energy randomization. This chemistry has little precedent, so that its mechanistic aspects are reviewed here to invite serious scrutiny.

Multiply protonated protein ions  $(M + nH)^{n+}$  formed by ESI should undergo electron capture at a protonated site, predicting initial formation of a hypervalent species such as  $R-NH_3^+$  (eq 2). Such neutral species have unusually low IE values of ~4 eV;<sup>18</sup> the presence of neighboring attractive cationic sites should raise this to 5–7 eV. Thus, capture of an electron should deposit a comparable amount of energy (ignoring the Franck–Condon factor) that could lead to energetic expulsion of  $H^+$  (eq 2) from the hypervalent site ( $R^{n+}-NH_3^+$  could also expel  $NH_3$ ; loss of  $NH_3$  is a minor dissociation pathway). Despite the ~6 eV of energy deposited initially, the ECD spectra of the  $(M + 4H)^{4+}$  ions of the 21-mer peptide (Figure 4) show  $[(M + 3H)^{3+}]/[(M + 4H)^{3+}] = 90\%$  while large (>~5 kDa) proteins show negligible  $H^+$  loss. For 11+ ubiquitin ions (Figure 2),  $[(M + 10H)^{10+}]/[(M + 11H)^{10+}] = <1\%$ , and their 8+ ions capture three electrons (Figure 3) to form  $(M + 8H)^{5+}$  with little  $H^+$  loss. The larger volume of large ions (denatured cytochrome *c*, 12.3 kDa, folds spontaneously in the gas phase)<sup>34</sup> should give improved efficiency for trapping excited  $H^+$  atoms, and the higher electrostatic charge should be more effective in slowing the escape of the polarizable  $H^+$  atom. Although in the ECD spectra of 5+, 4+,<sup>13a</sup> and 3+ mellitin (2.8 kDa) ions,  $[(M + (n - 1)H)^{(n-1)+}]/[(M + nH)^{(n-1)+}] = 50, 30,$  and 20%, respectively, when the  $H^+$  loss abundance is compared instead to that of all ECD product ions, the  $H^+$  loss ratios fall to 3,

4, and 18% because of the far higher lability of the more highly charged ions, as well as their higher attractiveness for  $H^+$ .

**Amide Backbone Cleavage.** Extensive evidence<sup>34,35</sup> indicates that the positively charged sites on the side chains are solvated by adjacent sites of favorable proton affinity, such as the numerous backbone carbonyl groups. For this, the  $H^+$  in effect is hydrogen-bonded between the folded-in side-chain functionality (of higher  $H^+$  affinity) and the carbonyl,  $R^{n+}-NH_2 \cdots H^+ \cdots O=C(R)-NHR'$ . Electron capture at this site produces the excited hypervalent species  $R^{n+}-NH_2 \cdots H^+ \cdots O=C(R')NHR'$ ; now the carbonyl group has a substantially higher  $H^+$  atom affinity than the side-chain functionality.<sup>13a</sup> Direct dissociation of this intermediate (eq 3) would then lead to the abundant ECD product ions, *c* and *z*.<sup>36</sup>

**ECD of –S–S–.** The spectrum of 10+ molecular ion of a 10 kDa protein containing one disulfide bond gave no products of eq 3 or 4, only the RSH and  $\cdot SR'$  of eq 5.<sup>13b</sup> However, the above mechanism would require solvation of the protonated side chain to the –S–S– group, whose proton affinity is 24 kcal mol<sup>–1</sup> less than that of the amide carbonyl, followed by electron capture at that site. Alternatively, the initial electron capture could produce a hypervalent species too energetic to retain the  $H^+$  atom; it would then explore the interior of the charged species, losing kinetic energy by collision, until it found a site of sufficiently high  $H^+$  affinity; that for the disulfide bond (eq 5) is 24 kcal mol<sup>–1</sup> higher than the amide carbonyl (eq 3).<sup>13b</sup> A further factor could increase the tendency for initial  $H^+$  loss within the ion. The solvated protonated site is forced outward in the multiply charged ion by the electrostatic repulsion of the other charges (~30 kcal mol<sup>–1</sup> for 13+ ions of cytochrome *c*);<sup>35</sup> neutralization relaxes this repulsion (the Franck–Condon factor), pulling the carbonyl group toward the interior and away from the newly formed  $H^+$  atom.

In a qualitative ordering of their  $H^+$  atom affinities, without –S–S– the favored site for  $H^+$  capture in proteins is tryptophan, apparently on the benzimidazole ring,<sup>13b</sup> followed by the amide carbonyl (eq 4) and the amide nitrogen (eq 3). Less abundant peaks represent the loss of small neutrals from  $(M + nH)^{(n-1)+}$ , consistent with lower  $H^+$  atom affinity at side-chain functionalities such as –SH (Cys), –NH<sub>2</sub> (Lys), and –OH (Ser, Thr). (Some of these small neutral losses could also occur by an alternative dissociation of the excited hypervalent species formed by  $e^-$  capture, such as loss of  $NH_3$  from  $R^{n+}-NH_3^+$  of eq 2.) Also indicative of the relatively low  $H^+$  affinity of hydroxyl and ether functionalities, the ECD spectrum of  $(M + H + K)^{2+}$  of  $\gamma$ -cyclodextrin,  $(C_6H_{10}O_5)_8$ , shows only an  $(M + K)^+$  ion; the released  $H^+$  is not captured.

The low  $H^+$  affinity of many common functionalities, such as those added in the posttranslational modifications of proteins, can make ECD spectra especially valuable for characterizing side chains that are easily lost in energetic ion dissociations such as CAD or IRMPD. Examples reported separately include  $\gamma$ -carboxy-

(34) McLafferty, F. W.; Guan, Z.; Haupt, U.; Wood, T. D.; Kelleher, N. L. *J. Am. Chem. Soc.* **1998**, *120*, 4732–4740.

(35) Schnier, P. D.; Gross, D. S.; Williams, E. R. *J. Am. Chem. Soc.* **1995**, *117*, 6747–6757.

(36) In comparison, the hydrogen atom departing from hypervalent oxonium radicals formed by the collisional neutralization of hexenyl methyl ethers appears to be trapped by an adjacent double bond, although H atom transfer was not detected for similar hypervalent ammonium radicals. (a) Shaffer, S. A.; Sadilek, M.; Turecek, F.; Hop, C. E. C. A. *Int. J. Mass Spectrom. Ion Processes* **1997**, *160*, 137–155. (b) Shaffer, S. A.; Wolken, J. K.; Turecek, F. *J. Am. Soc. Mass Spectrom.* **1997**, *8*, 1111–1123.

glutamic acid (CAD loss of CO<sub>2</sub>),<sup>37</sup> sulfated cysteine (CAD loss of SO<sub>3</sub>),<sup>37</sup> and N-glycosylated proteins (CAD loss of hexose).<sup>33</sup>

**Reactivity of the H<sup>•</sup> Captured Intermediate.** Theoretical calculations<sup>13b</sup> indicate that tryptophan should actually have a 4 kcal/mol higher H<sup>•</sup> affinity than the disulfide bond. Although the ECD backbone cleavage adjacent to Trp is 5 times more abundant than that induced by the other amino acids, the Trp cleavage is minor when the –S–S– moiety is present.<sup>13b</sup> The latter's H<sup>•</sup> capture intermediate, RSH–SR', has a negligible barrier for direct dissociation into RSH and ·SR', while backbone cleavage adjacent to H<sup>•</sup>-captured Trp must proceed through an entropically disfavored tight activated complex,<sup>13b</sup> so that loss of the captured H<sup>•</sup> could occur first.

However, the H<sup>•</sup> does not necessarily reach the distant –S–S– by capture and re-emission at other functionalities such as the carbonyl. With its high H<sup>•</sup> affinity, –S–S– should capture far "hotter" H<sup>•</sup> atoms than the amide carbonyl, suggesting that capture by them requires H<sup>•</sup> cooling by multiple collisions during exploration of the ion's interior.

An alternative to the intramolecular translocation of the released H<sup>•</sup> for capture at a distant –S–S– site is under further study. Solvation of a specific proton on a side chain is of high probability at a sterically favorable site of high proton affinity, but there will be a dynamic equilibrium of such solvated structures; when the protein dynamics happen to bring a solvated H<sup>+</sup> close to a disulfide linkage, the electron affinity of the partially protonated –S–S– will be substantially increased and a dissociative electron capture would presumably occur. This explanation would avoid both the complete proton transfer from a protonated amine to the disulfide, which we calculate to be very endothermic, and the need for long-range hydrogen atom migrations. It does, however, require that the captured electron be "stored" in some fashion prior to the disulfide cleavage so that neutralization can take place as soon as a favorable approach of a protonated amine to the disulfide occurs. Brauman has suggested that this storage could occur by generation of a high-*n* Rydberg state,<sup>13b</sup> which can be long-lived.<sup>38</sup>

The new model can be described in surface-crossing language. In the hypothetical Rydberg state, the lowest energy geometry is expected to be that with an intact –S–S– bond and a protonated amine. In the final state, the lowest energy geometry is calculated to be that corresponding to a –S<sup>•</sup>, a –SH, and the free amine. The neutralization can then be viewed as an avoided crossing between the Rydberg-state and final-state surfaces. If this were a general picture for all neutralization events, the barrier on the lower adiabatic surface could be expected to correlate with the H atom affinity of the functional group in question, in accord with our previously described experimental observations. The feasibility of this picture is being explored through the use of CASSCF calculations on two HS–SH + NH<sub>4</sub> surfaces. The first is cationic (44 total electrons) and is used as an approximation to the proposed high-*n* Rydberg state. The second is neutral (45 total electrons) and corresponds to the final state. The seam of intersection between these surfaces will correspond approximately to the avoided crossing described above. The question to be addressed is at what geometries this occurs and at what energy above the global minimum of the Rydberg state. The calculations necessary to answer those questions are in progress.

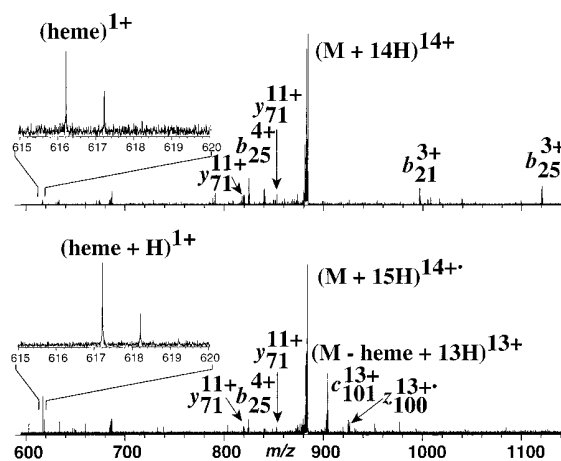


Figure 11. Top: partial CAD spectrum of ESI-generated (M + 14H)<sup>14+</sup> cytochrome c ions. Bottom: CAD spectrum of (M + 15H)<sup>14+</sup> radical ions from SWIFT isolation and ECD reduction of such (M + 15H)<sup>15+</sup> ions.

**Upper Mass Limit for ECD.** To date no ECD spectra have been obtained for proteins larger than 20 kDa. Although CAD is effective for far larger ions, the extent of backbone cleavage in CAD spectra also decreases with increasing protein size, reflecting the increasingly complex hydrogen-bonded tertiary structure. Dissociation methods (IRMPD, CAD, BIRD) that increase the ion's vibrational energy first cleave such noncovalent bonds before reaching an energy level sufficient for backbone bond rupture.<sup>39</sup> Limited collisional activation of deuterium-labeled cytochrome *c* ions can cause H/D scrambling without effecting backbone bond cleavage, but with ECD the H/D scrambling is minimal in the (M + *n*H)<sup>(*n*-1)+</sup> ions.<sup>13a</sup> Electron capture adds 5–7 eV to the ion; *c*, *z* cleavage (eq 3) requires ~2 eV,<sup>13b</sup> so the remainder can degrade the tertiary structure. If dissociation of the noncovalent bonds is too slow, the *c* and *z* products could recombine covalently to yield an ion of the same molecular weight as the precursor. Further efforts are in progress to pre-excite larger protein ions (e.g., "in-beam dissociation")<sup>13b</sup> to disrupt tertiary bonding and make ECD more effective for larger species.<sup>40</sup>

**Reduction of Fe<sup>3+</sup>.** Metalloproteins provide another example of unique product ions from ECD. It has been shown<sup>34</sup> that ESI of cytochrome *c* yields only the Fe<sup>3+</sup> form of the ion. ECD of its (M + 15H)<sup>15+</sup> ions gives the reduced (M + 15H)<sup>14+</sup> ions; CAD of these yields a (M – heme + 13H)<sup>13+</sup> ion that was much more intense (Figure 11) than that in the CAD spectrum of the nonreduced (M + 14H)<sup>14+</sup> ions. However, there is little heme loss in the 15+ ECD spectrum (no CAD), consistent with slow transfer of H<sup>•</sup> to the region of the less accessible Fe<sup>3+</sup> site. The CAD spectrum of the (M + 15H)<sup>14+</sup> ions (Figure 11) also contains a (heme + H)<sup>1+</sup>, *m* = 617, peak; CAD of the nonreduced (M + 14H)<sup>14+</sup> ion yields mainly the (heme)<sup>1+</sup> ion, *m* = 616. This

(37) Kelleher, N. L.; Zubarev, R. A.; Bush, K.; Furie, B.; Furie, B. C.; McLafferty, F. W.; Walsh, C. T. *Anal. Chem.* **1999**, *71*, 4250–4253.

(38) Held, A.; Schlag, E. W. *Acc. Chem. Res.* **1998**, *31*, 467–473.

(39) Speir, J. P.; Senko, M. W.; Little, D. P.; Loo, J. A.; McLafferty, F. W. *J. Mass Spectrom.* **1995**, *30*, 39–42. Little, D. P.; McLafferty, F. W. *J. Am. Soc. Mass Spectrom.* **1996**, *7*, 209–210. Fridriksson, E. K.; Baird, B. A.; McLafferty, F. W. *J. Am. Soc. Mass Spectrom.* **1999**, *10*, 453–455.

(40) Horn, D. M.; Lewis, M. A.; Ge, Y.; Zubarev, R. A.; Kruger, N. A.; McLafferty, F. W., in preparation.

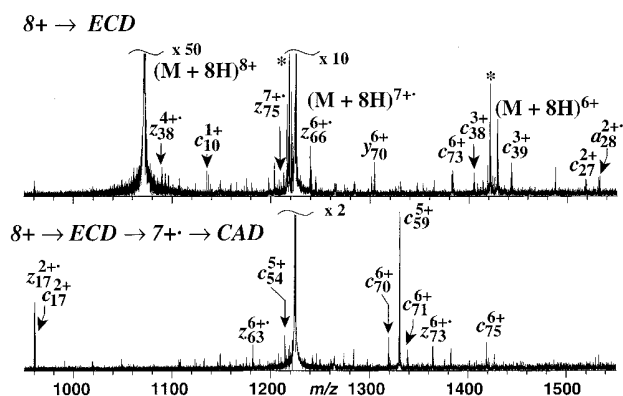
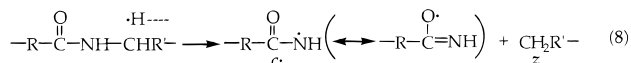


Figure 12. Top: ECD spectrum of bovine ubiquitin 8+ ions. Bottom: CAD spectrum of SWIFT-isolated, ECD-reduced  $(M + 8H)^{7+}$  radical ions.

apparent capture of  $H^+$  at the heme (not necessarily on the Fe atom itself) to yield  $Fe^{2+}$  heme is consistent with the  $\sim 20$  kcal/mol value calculated for the  $H^+$  atom affinity of  $Fe^{2+}$ .<sup>41</sup>

**CAD Spectra of  $(M + nH)^{(n-1)+}$  Reduced Species.** As illustrated for heme  $Fe^{3+}$  above, the most probable sites for the initial capture of the translational hot  $H^+$  are not necessarily the most favored on equilibration. For ubiquitin, the ECD products from the  $(M + 8H)^{8+}$  ions, presumably those from the fast dissociation of the initially formed  $(M + 8H)^{7+}$  ions, are substantially different from those of the CAD spectrum of the long-lived  $(M + 8H)^{7+}$  ions (Figure 12). IRMPD of  $(M + 8H)^{7+}$  gave a very similar spectrum. The CAD spectrum of  $(M + 7H)^{6+}$ , although less similar, was even less like the ECD spectra of either  $(M + 8H)^{8+}$  or  $(M + 7H)^{7+}$ . However, all of these CAD  $c$ ,  $z$  fragments are also observed in some abundance in the normal ECD spectra of other ubiquitin charge states. For ECD products of  $(M + 7H)^{7+}$  ions, the ostensible even-electron  $(M + 7H)^{5+}$  ions subjected to CAD did show low-abundance fragment ions such as  $(z_{47} + H)^{2+}$ , suggesting that the electrons are not completely paired; the CAD spectra of even-electron ubiquitin  $(M + nH)^{n+}$  ions for  $n \leq 7$  show almost no fragmentation, consistent with the higher bond dissociation energy of these even-electron species. In a similar fashion, the doubly reduced ECD products  $(M + 15H)^{13+}$  ions from 15+ cytochrome *c* precursors contributed significant products that are 1 Da higher in mass than those from  $(M - 15H)^{14+}$  (vide infra).

**Minor ECD Products.** In a small proportion of cases, the extra H atom goes to the  $C_a$  atom with formation of  $c^*$ ,  $z^*$  products, either by direct  $H^+$  capture (eq 8) or by H rearrangement. A pronounced



example is the difference in the ECD of the 4+ (Figure 4) and 3+ ions of the 21-mer peptide (Figure 13). In contrast to the 4+ precursors yielding the complementary pairs  $c_{10}^{1+}/z_{10}^{2+}$  and  $z_9^{1+}/c_{12}^{2+}$ , ECD of the 3+ yields the products  $c_{10}^{1+}$  and  $z_9^{1+}$ , along with (not shown) their complementary ions  $z_{11}^{1+}$  and  $c_{12}^{1+}$ . However, for these to result from eq 8 ostensibly requires  $H^+$

(41) For  $Fe-H^{2+}$  (quartet state)  $\rightarrow Fe^{2+}$  ( $^6D$ ) +  $H^+$ , using Gaussian 98 rev. A.6 at the UB3LYP/TZV level.

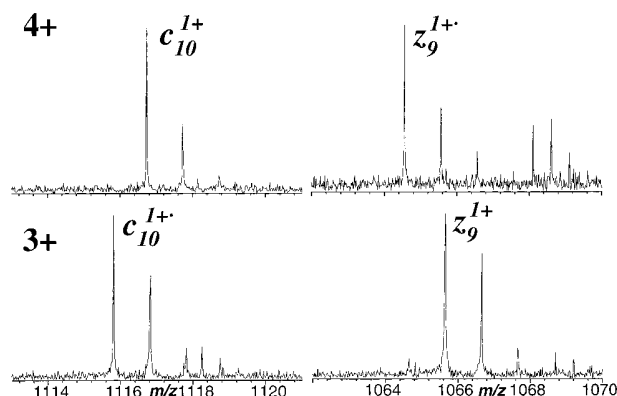


Figure 13. Formation of  $c$ ,  $z^*$  vs  $c^*$ ,  $z$  ions in ECD of the 21 mer of Figure 4. Top: ECD of 4+ ions; bottom, 3+ ions.

capture at Lys-11 for  $c_{10}^{1+}$  formation and at Asp-13 for  $c_{12}^{1+}$  formation, amino acids of very different reactivity. As shown extensively for unimolecular dissociation of odd-electron ions in electron ionization mass spectra,<sup>42</sup> the probability of rearranging zero, one, or even two hydrogen atoms is dependent on both enthalpic (product stability) and entropic (transition state) factors; these are under further investigation.

**Unit Dalton Differences in Product Masses.** Such an uncertainty in the mass of ECD backbone cleavage products ( $c \rightarrow c^*$ ,  $-1$  Da;  $z^* \rightarrow z$ ,  $+1$  Da) obviously is a problem in using ECD spectra for sequencing. Fortunately, this is uncommon for the ECD of peptide ions, especially those more highly charged, and this nearly disappears for ubiquitin and larger proteins. Also, as shown above, ECD spectra of peptides<sup>16</sup> (and mellitin, Figure 10)<sup>13a</sup> can show the loss of an  $H^+$  atom, presumably that from  $e^-$  neutralization of the protonated site; further dissociation of the  $H^+$  loss species would give  $H^+$ -deficient products, but fortunately,  $H^+$  loss is negligible in ECD of proteins of  $> 5$  kDa. ECD spectra of proteins do, however, have a greater tendency to show products with one or more extra hydrogen atoms due to multiple electron reduction. As discussed above, ECD from capture of a single electron reduces an  $H^+$ , so that the dissociating precursor  $(M + nH)^{(n-1)+}$  has an extra H versus its number of charges; its capture of a second  $e^-$  gives  $(M + nH)^{(n-2)+}$ , whose products could then contain two extra H atoms, one more than expected. With extensive exposure to electrons of the  $(M + 15H)^{15+}$  ions of cytochrome *c*, almost all product ions contained species with one or more extra H atoms. However, removal of the  $(M + 15H)^{13+}$  ions by on-resonance excitation during ECD gave nearly complete elimination of these anomalous products.<sup>43</sup> Secondary  $e^-$  capture by  $c$ ,  $z^*$  ions is also negligible.

**$MS^3$  with ECD.** Protein CAD spectra show internal (*i*) product ions from secondary dissociation of the terminal **b**, **y** primary products. Such *i* ions are negligible in the ECD spectra examined here, even though the  $c$  ions (eq 3) would appear to have the same basic structure as C-terminal amide peptides that show extensive ECD cleavages.<sup>16</sup> Capture cross sections are lower for the lower charge fragment ions; even if extended  $e^-$  capture eliminates the precursor molecular ions, their reduced forms will

(42) McLafferty, F. W.; Turecek, F. *Interpretation of Mass Spectra*, 4th ed.; University Science Books: Mill Valley, CA, 1993.

(43) Horn, D. M.; Zubarev, R. A.; McLafferty, F. W., manuscript in preparation.

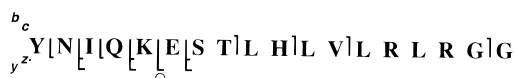


Figure 14. ECD (c, z•) and CAD (b, y) cleavages in SWIFT-isolated  $y_{18}^{3+}$  ions from IRMPD of ubiquitin 11+ ions.

be of high charge. Electron capture by z• ions would give an even-electron product. Most of our few attempts to obtain ECD spectra of ECD fragment ions have been unsuccessful. ECD of  $y_{58}^{8+}$  from nozzle–skimmer dissociation of ubiquitin cleaved 28 of its 57 interresidue bonds. The  $y_{18}^{3+}$  ions from IRMPD of ubiquitin were found to be unusually stable;<sup>5</sup> after SWIFT isolation, these ions gave an ECD spectrum (Figure 14) with four c and five z• products, but with no complementary pairs. CAD gave only four y ions; only one represented cleavage between an amino acid pair not separated in the ECD spectrum.

**Nonergodic Cleavage.** There appears to be little precedent for this additional aspect of the ECD mechanism. Dissociation without equilibration of the vibrational energy has been reported only in small species.<sup>44</sup> To summarize the evidence for nonergodic dissociation from e<sup>-</sup> capture by protein ions, the 5–7 eV of added energy would represent only millivolts per bond if randomized in a protein, and yet small differences in backbone bond dissociation energies cause far less discrimination in cleavage by ECD than by CAD/IRMPD. Low-energy competing reactions, such as H/D scrambling, are suppressed far more effectively in ECD than in CAD/IRMPD. Capture of a lower energy electron, such as from SF<sub>6</sub><sup>-</sup>, does not give c, z• products. RRKM calculations on the simple system HO–C\*(CH<sub>3</sub>)–NH–CH<sub>3</sub> predict that the •CH<sub>3</sub> loss corresponding to eq 3 has a rate constant of  $k > 10^{12} \text{ s}^{-1}$ ,<sup>13b</sup> faster than vibrational energy transfer.

## CONCLUSIONS

Although at present ECD appears most suitable for ESI multiply charged ions trapped in an FTMS instrument, the high

(44) Schlag, E. W.; Levine, R. D. *Chem. Phys. Lett.* **1989**, *163*, 523–530. Dian, E. W.-G.; Herek, J. L.; Kim, Z. H.; Zewail, A. H. *Science* **1998**, *279*, 847–851.

ECD efficiencies now achievable extend MS/MS capabilities for extensive sequencing of mixture components by nearly 1 order of magnitude in molecular weight. Full sequence information can be obtained from ECD and CAD spectra of mellitin (Figure 10) and ubiquitin using a computer algorithms to be reported separately.<sup>43</sup> The top down sequencing strategy<sup>14</sup> for much larger proteins would involve degrading these (CAD, proteolysis) to fragment ions of ~10 kDa size for ECD sequencing, with fragment ordering from the masses of the overlapping protein products. Further, information on posttranslational modifications is preserved far better than it is in CAD or IRMPD spectra. A useful CAD spectrum of a 29 kDa protein has been obtained from 10<sup>-17</sup> mol of sample;<sup>3a</sup> it is conceivable that ECD/CAD spectra of 10<sup>-15</sup> mol of protein can provide nearly complete sequences.

Such a simple way to form odd-electron ions of large species also opens up basic research on their chemistry reminiscent of the extensive studies of radical site reactions in electron ionization mass spectra.<sup>42</sup> Further reactions, both intra- and intermolecular, of such ECD odd-electron ions are under investigation, as are ECD spectra of multiply charged cations containing other functionalities.

## ACKNOWLEDGMENT

We thank Barbara Baird, Tadhg Begley, John Brauman, Blas Cerda, H. Floyd Davis, Scott Gronert, Ziqiang Guan, Katherine Hunt, Hélène Lavanant, Carl Lineberger, Piotr Piecuch, Michael Senko, Frantisek Turecek, Julian Whitelegge, and Brian Winger for valuable discussions, Ted Thannhauser and Hannah Gould for samples, and the National Institutes of Health (Grant GM16609 for F.W.M.), the National Science Foundation (Grant CHE-9876387 to B.K.C.), and Perkin-Elmer Corp. (ACS Division of Analytical Chemistry Fellowship to N.L.K.) for generous funding.

Received for review July 22, 1999. Accepted November 16, 1999.

AC990811P